IOPscience iopscience.iop.org

Home Search Collections Journals About Contact us My IOPscience

Enhancement of electrical and ferromagnetic properties by additional Al doping in Co:ZnO thin films

This article has been downloaded from IOPscience. Please scroll down to see the full text article.

2007 J. Phys.: Condens. Matter 19 296208

(http://iopscience.iop.org/0953-8984/19/29/296208)

View the table of contents for this issue, or go to the journal homepage for more

Download details:
IP Address: 129.252.86.83
The article was downloaded on 28/05/2010 at 19:50

Please note that terms and conditions apply.

J. Phys.: Condens. Matter **19** (2007) 296208 (10pp)   doi:10.1088/0953-8984/19/29/296208

Enhancement of electrical and ferromagnetic properties by additional Al doping in Co:ZnO thin films

X J Liu, C Song, F Zeng and F Pan

Laboratory of Advanced Materials, Department of Materials Science and Engineering, Tsinghua University, Beijing 100084, People's Republic of China

E-mail: panf@mail.tsinghua.edu.cn

Received 28 March 2007, in final form 4 June 2007
Published 5 July 2007
Online at stacks.iop.org/JPhysCM/19/296208

Abstract
Several properties of Al-doped $Zn_{0.95}Co_{0.05}O$ thin films prepared by radio frequency (RF) magnetron co-sputtering have been systematically investigated. The experimental results indicate that Co^{2+} steadily substitutes for tetrahedrally coordinated Zn^{2+} in the ZnO wurtzite lattice without any segregated secondary phase formation, and that a trace amount of additional Al doping has a profound influence on the enhancement of electrical and magnetic properties of Co:ZnO films. All the films show room-temperature ferromagnetism, and a giant magnetic moment of 3.36 μ_B/Co is obtained in the $Zn_{0.948}Co_{0.05}Al_{0.002}O$ thin film. The ferromagnetic ordering is seen to be correlated with the structural defects. Moreover, a phenomenon of band gap broadening and absorption edge blueshift can be achieved by additional Al doping into the Co:ZnO films.

1. Introduction

Diluted magnetic semiconductors (DMSs) with Curie temperature at or preferably above room temperature (RT) have attracted much attention for their potential use in spintronic devices [1]. Following the prediction of Dietl *et al* which suggests that RT ferromagnetism (FM) may exist in wide band gap semiconductors [2], ZnO doped with transition metals has been studied extensively. Despite intensive efforts having been made on ZnO-based DMS thin films, the experimental results do not converge to a definite conclusion [3, 4]. The origin of FM in these materials is still a matter of strong debate. The currently accepted picture for the FM in DMSs is that the presence of carriers is essential to mediate the interaction between the magnetic ions. Through an analysis of density functional calculations, Sluiter *et al* have shown that both electron doping with zinc interstitials (Zn_i) and hole doping with zinc vacancies (V_{Zn}) make a Co:ZnO sample strongly ferromagnetic [5]. Therefore, some works have been done with additional dopants to enhance or induce FM [6, 7]. In the case of (Co, Al)-codoped ZnO

powders, Liu *et al* have found that the high-temperature FM can be obtained through increasing the carrier concentration which is realized by doping a few per cent of Al [7], while Alaria *et al* have shown that the creation of n-type free carriers is not sufficient to create ferromagnetic interactions [8]. It is hence of vital importance to clarify whether the RT FM is intrinsically linked to the free-carrier concentration. In addition to the carrier codoping effect, there are recent predictions, not fully resolved at the present time, realizing the importance of structural defects for ferromagnetic ordering in DMSs [4, 9, 10]. Hong *et al* highlight in recent papers the role of defects in tuning the FM in DMS oxide films [11, 12], while Jayakumar *et al* also report the influence of defects on the enhanced ferromagnetic properties in codoping oxide systems [13]. In view of this, we think it worthwhile to explore the correlations between FM and free carriers or structural defects introduced by additional doping, which is of help for a better understanding of the intrinsic FM in DMSs.

In this work, many experiments are used to study the structural, optical, electrical and magnetic properties of Al-doped $Zn_{0.95}Co_{0.05}O$ thin films. It is found that a trace amount of additional Al doping plays an important role in the enhancement of the electrical and ferromagnetic properties of Co:ZnO films, and the carrier concentration is important, as expected for DMSs, but that the electrons are not the only mediators of ferromagnetic exchange. The RT FM is more likely ascribed to the structural defects. It should be pointed out that a giant magnetic moment of 3.36 μ_B/Co is obtained at RT in $Zn_{0.948}Co_{0.05}Al_{0.002}O$ thin film, in contrast to 1.70 μ_B/Co in $Zn_{0.95}Co_{0.05}O$ thin film.

2. Experiment

$Zn_{0.95-x}Co_{0.05}Al_xO$ ($x = 0, 0.001, 0.002, 0.004, 0.005$) thin films were deposited on Si(100) and quartz glass substrates at RT by RF magnetron co-sputtering. The films grown on quartz glass substrates were used to measure the transmittance spectra. Co and Al chips were attached on a ZnO target (99.99%), which was used to control the compositions of Co and Al. The base pressure of the deposition chamber was $\sim 7 \times 10^{-4}$ Pa. Deposition was performed in a 0.8 Pa argon atmosphere. At a deposition power of ~260 W, the deposition rate was ~ 0.038 nm s^{-1}.

The structure and crystalline quality of the samples were examined with θ–2θ x-ray diffraction (XRD) using Cu Kα radiation. The compositions of the films were determined by x-ray fluorescence (XRF). X-ray photoelectron spectroscopy (XPS) was used to verify the Co compositions of the films and characterize the chemical valence of Co atoms. Scanning electron microscopy (SEM) and high-resolution transmission electron microscopy (HRTEM) were used to study the structural characteristics, interface bonding and grain boundaries of the films. The x-ray absorption near-edge spectrum (XANES) at the Co K edge was measured to confirm the valence state of the Co dopant in the ZnO lattice throughout the films. RT optical transmittance spectra measurements were made on an ultraviolet–visible spectrophotometer in the wavelength range from 300 to 800 nm. Magnetic properties were examined with a vibrating sample magnetometer (VSM) at RT. After the magnetic measurements, samples were taken to determine the Co content using induced-coupled-plasma (ICP) atomic emission spectra so as to calculate the magnetic moment per Co ion. The electrical properties of the films were investigated by four-point probe and Van der Pauw Hall measurements at RT.

3. Results and discussion

The structures of the $Zn_{0.95-x}Co_{0.05}Al_xO$ thin films on Si(100) substrates were examined by XRD. All the films have a single ZnO wurtzite structure with c-axis preferred orientations, and no diffraction peaks attributed to Co- or Al-related secondary phases were detected within the

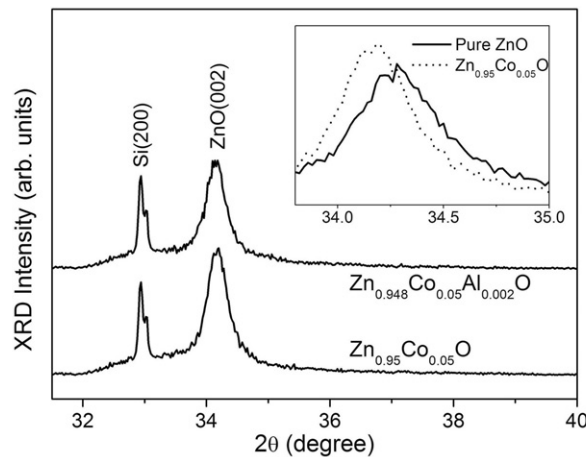

Figure 1. XRD patterns of $Zn_{0.95-x}Co_{0.05}Al_xO$ ($x = 0, 0.002$) thin films on Si(100) substrates. The inset shows a comparison of (002) reflections of $Zn_{0.95}Co_{0.05}O$ (dotted line) and the pure ZnO (solid line).

sensitivity of the XRD measurements. Figure 1 depicts the XRD spectra of $Zn_{0.95-x}Co_{0.05}Al_xO$ ($x = 0, 0.002$) thin films with 2θ ranging from 31.5° to 40°. It is obvious that the peak corresponding to ZnO (002) changes little except for the decrease of intensity after additional Al doping in $Zn_{0.95}Co_{0.05}O$ thin film, implying the decline of crystalline quality with a trace amount of Al doping. The inset of figure 1 compares the peaks for $Zn_{0.95}Co_{0.05}O$ and pure ZnO films. The relative shift of the (002) peak to a lower angle for the $Zn_{0.95}Co_{0.05}O$ thin film indicates that Co atoms incorporate into the wurtzite lattice of ZnO.

Detailed atomic-scale characterization was done using SEM and HRTEM to investigate the microstructural characteristics of the films and the possibility of nanoclustering or secondary phase formation, which might not be detected by XRD. The surface morphology and typical cross-sectional HRTEM images of the $Zn_{0.948}Co_{0.05}Al_{0.002}O$ thin film are shown in figure 2. The surface of the film is very smooth with dense grains and uniform dimension, and no visible defects are observed, as shown in figure 2(a). It is clear in figure 2(b) that the thin film has a thickness of ~90 nm, with columnar growth structure. The higher magnification in figure 2(c) shows that the film is a nanoscale polycrystalline structure. A representative {001} oriented crystal grain is marked by two arrows. That is, the area between the two arrows is a ~15 nm diameter columnar grain. The interplanar distance of fringes is measured to be 0.26 nm, which corresponds to the spacing of (002) planes of wurtzite ZnO. This is in good agreement with the XRD result. Even though structural defects marked as A, B, C, and D can be clearly observed in figure 2(d), there is no evidence for the presence of secondary phases in the grain boundary areas. Figure 2(e) shows the area of interface between the film and the substrate. There is a thin layer of native oxide (~2.5 nm) underneath the film. Various crystal orientations denoted by white arrows indicate that the film grows randomly initially. More interestingly, though the film show apparent columnar structure at a distance from interface (shown in figure 2(c)), the film grows in the form of small grains at the area near surface, which is shown in figure 2(f). The distinct interlayer is for the growth transition from the columnar structure to small grains. Similarly, there is no observation for the presence of Co- or Al-related secondary phases in these areas. Based on the randomicity of the selective detected area, it could be concluded that Co ions incorporate into the wurtzite structure of ZnO without any Co-

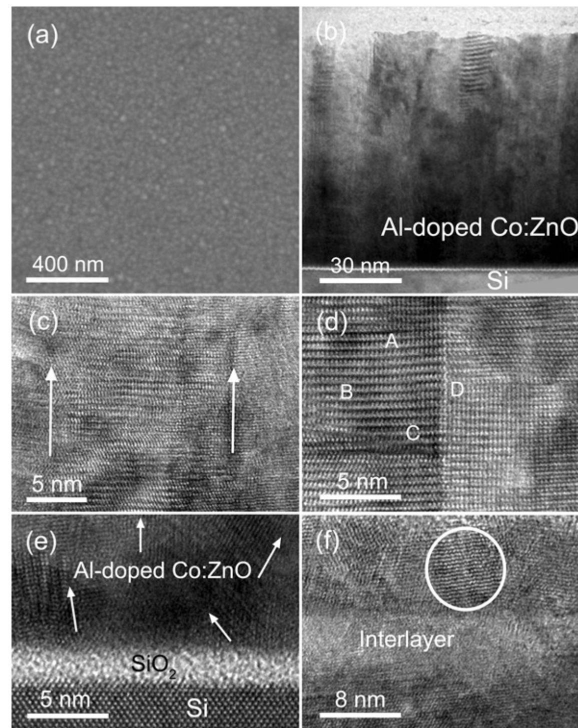

Figure 2. (a) SEM image and (b) a low-magnification cross-section HRTEM image of the $Zn_{0.948}Co_{0.05}Al_{0.002}O$ thin film. Typical cross-sectional HRTEM image of (c) a representative {001} oriented crystal grain, (d) the area near grain boundary, (e) the interface between the film and the substrate, and (f) the area near the surface of the film. The white arrows mark the boundaries of the crystal grains. The white circle represents a small crystal grain at the area near the surface of the film. A, B, C, and D denote the structural defects in the film.

related secondary phase formation, and that numerous structural defects are present in the grain boundary areas.

In order to characterize the charge state of the Co ions in the films, Co 2p XPS spectra for $Zn_{0.95-x}Co_{0.05}Al_xO$ ($x = 0, 0.002$) thin films are shown as figure 3. It is apparent that the peak positions of Co $2p_{3/2}$, Co $2p_{1/2}$, and corresponding satellites for $Zn_{0.95-x}Co_{0.05}Al_xO$ ($x = 0, 0.002$) thin films are almost the same, indicating that a trace amount of Al doping has a negligible influence on the state of Co ions, and that Co ions are uniform and stable in the Co:ZnO thin films. The Co $2p_{3/2}$ peak position located at 780.8 eV is quite different from that of Co metal (778.3 eV), implying that any Co occurrence should therefore be below the sensitivity of the technique. The energy difference between Co $2p_{3/2}$ and $2p_{1/2}$ ($\sim$796.3 eV) core levels is 15.5 eV, which is consistent with that of Co^{2+} in the literature [14], indicating that Co ions have a valence of 2+ in Co:ZnO films. It is expected that Co^{2+} would incorporate into the wurtzite lattice and substitute for the sites of Zn^{2+} since the ionic radius of Co^{2+} (0.58 Å) is relatively close to that for Zn^{2+} (0.60 Å), differing by only 3.3%, and Co^{2+} is very soluble in ZnO [15].

Nevertheless, it is difficult to confirm whether or not Co precipitates exist in the area beyond the detection limit of XPS and the Co^{2+} state in XPS comes from the substitutional behaviour of Co at Zn sites. Hence Co K-edge XANES was carried out to solve the problem, because it can detect all the way to the interface due to the long penetration depth of high-energy

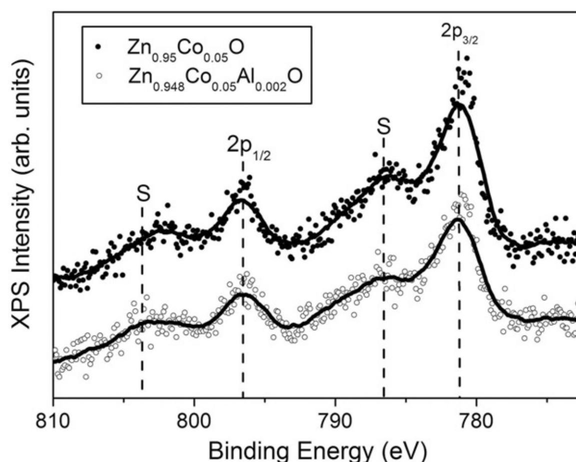

Figure 3. Co 2p XPS spectra for $Zn_{0.95-x}Co_{0.05}Al_xO$ ($x = 0, 0.002$) thin films. S denotes satellite peaks. Solid lines show a smoothing of the data.

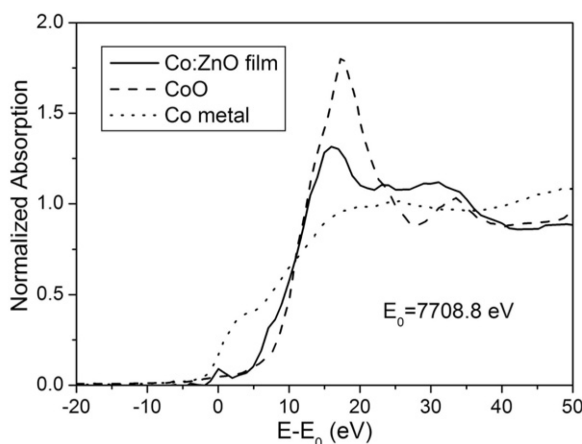

Figure 4. Co K-edge XANES spectra for $Zn_{0.95}Co_{0.05}O$ film with reference samples: Co metal and CoO.

x-rays, and is very sensitive to the charge state of Co. As shown in figure 4, metallic cobalt shows a distinct broad K-edge absorption feature at $E - E_0 = 3$ eV ($E_0 = 7708.8$ eV) which is unique to Co^0 and can be effectively used to determine the presence of Co metal. However, it is not present in the spectrum of the Co:ZnO film. For comparison, the Co K-edge spectrum of Co:ZnO film shows the signature 1s $\rightarrow$ 3d pre-edge absorption of substitutional Co^{2+} in ZnO at $E - E_0 = 0.2$ eV, that is, Co is coordinated to O ligands and Co 3d/O 2p mixing occurs in low-lying conduction-band states [16]. In addition, the obvious difference of the XANES spectra between Co:ZnO film and CoO indicates that Co incorporates into the wurtzite lattice of ZnO instead of in the CoO form. Therefore from the comparison of Co K-edge spectra it can be concluded that there is no evidence of Co precipitates throughout the film and Co^{2+} substitutes for Zn^{2+} in the lattice.

Typical optical transmittance spectra of pure ZnO and $Zn_{0.95-x}Co_{0.05}Al_xO$ thin films recorded in the wavelength region of 300–800 nm are shown in figure 5(a). The films are

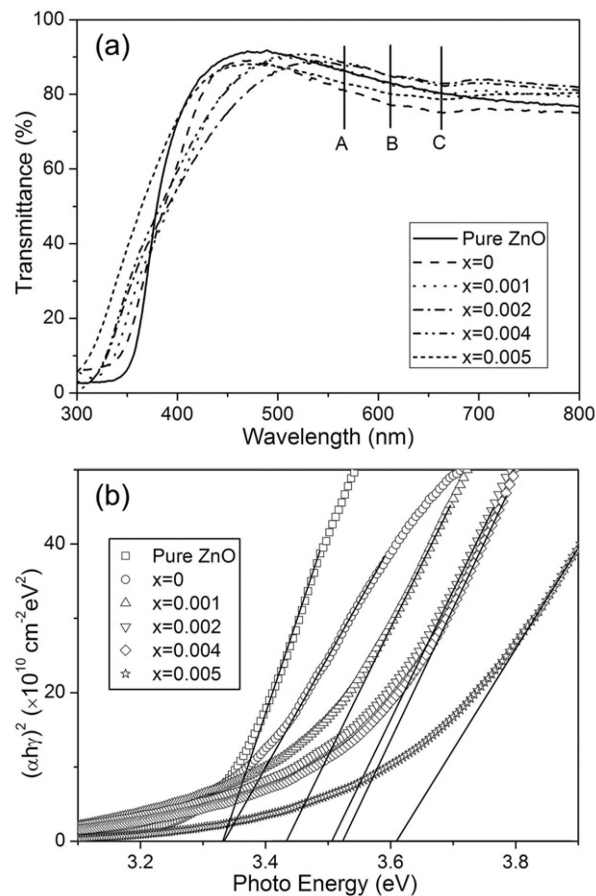

Figure 5. (a) Optical transmittance spectra of the pure ZnO and $Zn_{0.95-x}Co_{0.05}Al_xO$ thin films. (b) E_g of the pure ZnO and $Zn_{0.95-x}Co_{0.05}Al_xO$ thin films derived from transmittance spectra.

transparent to visible light with an average transmittance value of >80%, indicating a good optical quality with low scattering or absorption losses. Clearly, the transmission is found to be maximum for pure ZnO thin film and varies with the additional Al concentration. The change of optical transmission is associated with the loss of light due to oxygen vacancies (V_O) and scattering at grain boundaries [17]. Moreover, the relative sharp absorption edge observed for pure ZnO film at ∼373 nm is found to start broadening with additional Al doping, which suggests an increase in the disorder in Co:ZnO film with incorporation of Al and is in agreement with XRD analysis as discussed earlier. Besides, with the increase in Al concentration, the absorption edge shows a continuous blueshift. Furthermore, three other slight peaks around 565, 611, and 661 nm, denoted as A, B, and C, are observed in visible light wavelength for $Zn_{0.95-x}Co_{0.05}Al_xO$ thin films, which are correlated with the d–d transitions of the tetrahedrally coordinated Co^{2+} ions and attributed to the $^4A_2(F) \rightarrow {}^2A(G)$, $^4A_2(F) \rightarrow {}^4T_1(P)$, and $^4A_2(F) \rightarrow {}^2E(G)$, respectively [7, 18]. This, together with the results of foregoing analytical methods, supports the conclusion that Co is incorporated into the lattice of ZnO, as Co^{2+} substituting for Zn^{2+} ions, forming a solid solution with wurtzite structure instead of Co precipitates.

Table 1. The electrical and magnetic properties of $Zn_{0.95-x}Co_{0.05}Al_xO$ thin films. C_{Al}, n_e and n_{Al} represent the Al concentration (at.%), carrier concentration (cm^{-3}) and Al density (cm^{-3}), respectively.

C_{Al} (at.%)	Resistivity (Ω cm)	Hall mobility (cm^2 V^{-1} s^{-1})	n_e (cm^{-3})	n_e/n_{Al}	M_s (μ_B/Co)
0.0	1.267	14.0	3.790×10^{17}	—	1.70
0.1	2.698×10^{-2}	6.0	4.597×10^{19}	1.09	2.71
0.2	3.985×10^{-3}	7.0	2.500×10^{20}	2.98	3.36
0.4	1.036×10^{-2}	4.0	1.597×10^{20}	0.95	2.34
0.5	7.334×10^{-2}	4.0	2.229×10^{20}	1.06	2.76

It is well known that ZnO-based film, being a wide band gap semiconductor, has an absorption coefficient (α), which obeys the following relation for high-photon energies [19]:

$$(\alpha h\gamma)^2 = A(h\gamma - E_g) \tag{1}$$

where E_g is the optical band gap of the thin film, h is Planck's constant, γ is the frequency of the incident photon, $h\gamma$ is the energy of excitation, and A is a constant. The absorption coefficient (α) of the film is determined from the transmittance data using the following relation [19]:

$$\alpha = [2.303 \log(1/T)]/d \tag{2}$$

where T is the transmittance and d is the thickness of the film. The plots of $(\alpha h\gamma)^2$ versus energy $h\gamma$ for all the films are shown in figure 5(b). The band gap energy is obtained by extrapolating the linear part of the plot curves to intercept the energy axis (at $\alpha h\gamma = 0$). The measured direct band gap energy of the pure ZnO and $Zn_{0.95-x}Co_{0.05}Al_xO$ ($x = 0, 0.001, 0.002, 0.004, 0.005$) films is 3.33, 3.33, 3.43, 3.51, 3.53, and 3.61 eV, respectively. It is clear that the value of E_g of $Zn_{0.95-x}Co_{0.05}Al_xO$ films increases with the increase in Al concentration. This phenomenon is well explained in terms of the so-called Burstein–Moss effect that the Fermi level merges into the conduction band with the increase in carrier concentration [20]. Based on the analysis above, we can draw the conclusion that a widened band gap can be achieved by additional Al doping into the Co:ZnO films, and that the band gap can be controlled by changing the Al concentration.

The results of Hall measurements are summarized in table 1. It is found that a trace amount of additional Al doping has a profound influence on the electrical properties of Co:ZnO films. The resistivity (Ω cm) of the films obviously decreases from 1.267 ($x = 0$) to 3.985×10^{-3} ($x = 0.002$) and then slightly increases to 7.334×10^{-2} with further increase in Al concentration to 0.005, while the Hall mobility (cm^2 V^{-1} s^{-1}) slightly decreases from 14.0 to 4.0 by additional Al doping. The electron concentration (n_e) is 3.790×10^{17} cm^{-3} for the film of $Zn_{0.95}Co_{0.05}O$ and then reaches 1.597–2.500×10^{20} cm^{-3} with a trace amount of Al doping. Figure 6 shows the dependence of electron carrier concentration of Al-doped $Zn_{0.95}Co_{0.05}O$ thin films on additional Al concentration. It is noted that the n_e dramatically increases up to $x = 0.002$ at first and is then in the state of saturation with further increase in Al concentration, implying that Al is not the only candidate to introduce electron carriers. It is well known that ZnO is very easily and naturally an n-type semiconductor because of the existence of native defects such as V_O and Zn_i. In our Al-doped $Zn_{0.95}Co_{0.05}O$ thin films, a number of structural defects can be formed at the grain boundary areas due to the additional Al doping during deposition, which could enhance the concentrations of point defects, for instance V_O and Zn_i, in the films. The enhancive point defects as well as the native defects are regarded as another form of primary donor to supply electron carriers.

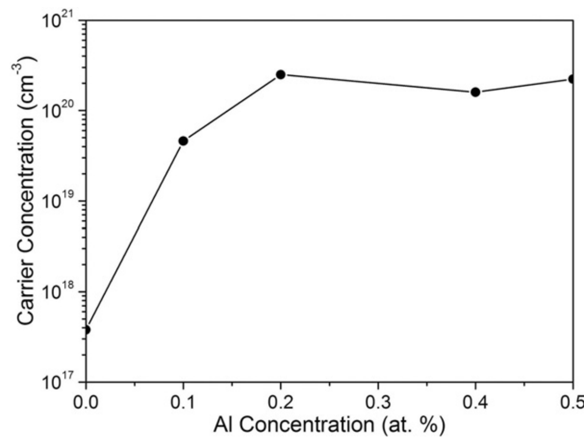

Figure 6. Al concentration dependence of electron carrier concentration in Al-doped $Zn_{0.95}Co_{0.05}O$ thin films.

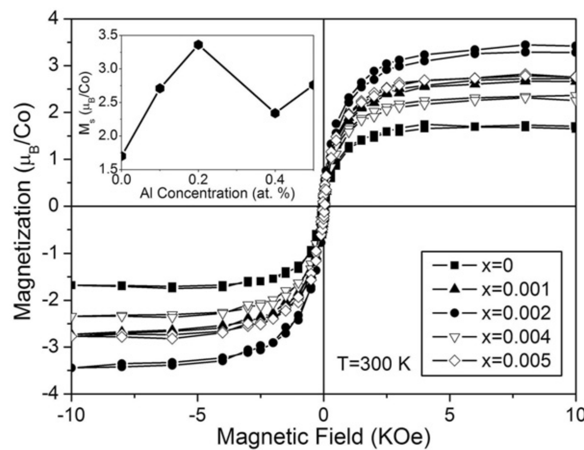

Figure 7. Magnetization hysteresis curves of $Zn_{0.95-x}Co_{0.05}Al_xO$ thin films measured at RT. The inset shows the Al concentration dependence of saturation magnetization.

Magnetization measurements display a distinct ferromagnetic behaviour. Figure 7 shows the magnetization versus magnetic field (M–H) curves of the $Zn_{0.95-x}Co_{0.05}Al_xO$ thin films. It is useful to mention here that the magnetic background of the substrate has been subtracted from all of the magnetization data. ICP is used to measure the effective cobalt numbers in the samples after the measurement of the magnetic properties to calculate the average magnetic moment per Co atom. The Al concentration dependence of saturation magnetization (M_s) is shown in the inset, while the values of M_s are compiled in table 1. Apparently, all the loops show the features of FM at RT (∼300 K), indicating the Curie temperature of the $Zn_{0.95-x}Co_{0.05}Al_xO$ thin film is well above RT. The most interesting result here is that a trace amount of additional Al doping can enhance the magnetic moment per Co ion of the Co:ZnO films, and that a robust M_s of 3.36 μ_B/Co (μ_B = Bohr magneton) is obtained for the film of $Zn_{0.948}Co_{0.05}Al_{0.002}O$, much larger than that of $Zn_{0.95}Co_{0.05}O$ film (1.70 μ_B/Co) without Al doping. That is, the carrier concentration jumps three orders of magnitude and the effective M_s is found to approach full polarization, approximate doubling with small Al additions. Simultaneously, samples

with Al concentrations of 0.001, 0.004 and 0.005 show M_s of 2.71, 2.34 and 2.76 μ_B/Co, corresponding to an n_e of 4.597×10^{19}, 1.597×10^{20} and 2.229×10^{20} cm^{-3}, respectively.

The increase in M_s with additional Al doping, combined with the increase in n_e, implies that the free-carrier concentration is important, as expected for DMSs. It is possible that the FM observed in the samples originates from the carrier-mediated mechanism, in which the presence of Co^{2+} ions influences the free-carrier behaviour through the sp–d exchange interaction between the localized magnetic moments and the spins of the itinerant carriers [21]. However, it should be noted here that n_e (1.597×10^{20} cm^{-3}) is larger whereas M_s (2.34 μ_B/Co) is smaller for the film of $Zn_{0.95-x}Co_{0.05}Al_xO$ ($x = 0.004$), compared with those of $Zn_{0.95-x}Co_{0.05}Al_xO$ ($x = 0.001$) ($n_e = 4.597 \times 10^{19}$ cm^{-3}, $M_s = 2.71$ μ_B/Co), indicating the electrons are not the only mediators of ferromagnetic exchange, similar to the result reported by Xu *et al* [22].

In terms of substitutions, this curious result is likely more easily understood when taking into account the existence of donor defects. From the analysis above, it is clear that the additional Al doping leads to the decline of crystalline quality and the diminishing of the crystal grains of Co:ZnO films, together with which a large number of structural defects are introduced and mainly located at the grain boundary areas in our samples. Along with this, the concentration of donor defects (notably V_O and Zn_i) is increased to a certain extent. Since the free electrons can be introduced into Co:ZnO films not only by additional Al doping but also by enhancive donor defects, the ratio of the carrier concentration to the Al density (n_e/n_{Al}) is an indirect measure to show the amount of defects in the films. That is, based on the condition that the Al concentration is very small, which ensures the absolute solution of Al and the same contribution per Al atom to the enhancement of n_e, the larger value of n_e/n_{Al} means a greater amount of donor defects in the films. Apparently, the n_e/n_{Al} (1.09) of $Zn_{0.95-x}Co_{0.05}Al_xO$ ($x = 0.001$) is larger than that of $Zn_{0.95-x}Co_{0.05}Al_xO$ ($x = 0.004$) ($n_e/n_{Al} = 0.95$), implying more donor defects in $Zn_{0.949}Co_{0.05}Al_{0.001}O$ films, corresponding to the stronger M_s of 2.71 μ_B/Co. Therefore, the coupling between Co ions through donor defects seems to play a critical role in governing the ferromagnetic ordering, which can reasonably explain the observed RT FM in some highly insulating oxides [23, 24]. Moreover, our other work has also demonstrated that the structural defects are strongly correlated with the RT FM in Co:ZnO films, and that the carriers involved in carrier-mediated exchange are natural by-products of the creation of the defects [25].

Now that the presence of Co precipitates is ruled out by various measurements, the ferromagnetic ordering is indeed intrinsic to Co:ZnO films based on the substitutional behaviour of Co in the wurtzite lattice of ZnO, and the donor defects as well as the electrons are important to the enhancement of FM. Our experimental results are consistent with the reports by Coey and co-workers [24, 26]. In their studies, the RT ferromagnetic exchange in diluted magnetic oxides is mediated by shallow donor electrons that form bound magnetic polarons (BMPs), which overlap to create a spin-split impurity band, and the nature of the defects is responsible for the shallow donors. In more detail, recent reports have confirmed that oxygen vacancies (V_O) can enhance the RT FM and that a small level of Zn_i plays a crucial role in mediating the FM in Co:ZnO films, and that the presence of a large concentration of donor defects allows for long-range FM in accordance with the BMP model [4, 11, 23, 26]. A similar situation may also be present in our Co:ZnO films. On the basis of the BMP model, the donor spin of a defect strongly correlating with Co^{2+} within its orbit mediates effective interactions between them based on a Heisenberg exchange Hamiltonian, and the shaped BMPs try to sufficiently spread out to overlap and interact with adjacent BMPs to realize magnetic ordering. With additional Al doping, more induced donor defects will be produced and the ferromagnetic coupling interactions appear to be more effective and then consequently enhance the ferromagnetic properties of Co:ZnO films.

4. Conclusion

In conclusion, RT ferromagnetic $Zn_{0.95-x}Co_{0.05}Al_xO$ thin films with *c*-axis orientation are prepared by RF magnetron co-sputtering. The experimental results indicate that the Co ions steadily substitute for tetrahedrally coordinated Zn cations in the ZnO wurtzite lattice and exhibit a +2 oxidation state. There is no evidence for the formation of any segregated secondary phases, while a large number of structural defects can be observed in the areas of grain boundaries with a trace amount of Al doping. Besides the contribution of carrier concentration to the ferromagnetic interaction, it appears that the structural defects are of importance in mediating RT FM in ZnO-based semiconductors. In addition, the increase in carrier concentration is more likely related to the broadening of optical band gap.

Acknowledgments

The authors express their thanks for the financial support from the National Natural Science Foundation of China (No. 50325105, 50371040) and the Ministry of Science and Technology of China.

References

[1] Ohno H 1998 *Science* **281** 951
[2] Dietl T, Ohno H and Matsukura F 2001 *Phys. Rev.* B **63** 195205
[3] Zhu T, Zhan W S, Wang W G and Xiao J Q 2006 *Appl. Phys. Lett.* **89** 022508
[4] Khare N, Kappers M J, Wei M, Blamire M G and MacManus-Driscoll J L 2006 *Adv. Mater.* **18** 1449
[5] Sluiter M H F, Kawazoe Y, Sharma P, Inoue A, Raju A R, Rout C and Waghmare U V 2005 *Phys. Rev. Lett.* **94** 187204
[6] Lin H T, Chin T S, Shih J C, Lin S H, Hong T M, Huang R T, Chen F R and Kai J J 2004 *Appl. Phys. Lett.* **85** 621
[7] Liu X C, Shi E W, Chen Z Z, Huang H W, Xiao B and Song L X 2006 *Appl. Phys. Lett.* **88** 252503
[8] Alaria J, Bieber H, Colis S, Schmerber G and Dinia A 2006 *Appl. Phys. Lett.* **88** 112503
[9] Coey J M D 2005 *J. Appl. Phys.* **97** 10D313
[10] Archer P I and Gamelin D R 2006 *J. Appl. Phys.* **99** 08M107
[11] Hong N H, Sakai J, Huong N T, Poirot N and Ruyter A 2005 *Phys. Rev.* B **72** 045336
[12] Hong N H, Sakai J and Brizé V 2007 *J. Phys.: Condens. Matter* **19** 036219
[13] Jayakumar O D, Gopalakrishnan I K and Kulshreshtha S K 2006 *Adv. Mater.* **18** 1857
[14] Yin Z, Chen N, Chai C and Yang F 2004 *J. Appl. Phys.* **96** 5093
[15] Jin Z, Murakami M, Fukumura T, Matsumoto Y, Ohtomo A, Kawasaki M and Koinuma H 2000 *J. Cryst. Growth* **214/215** 55
[16] Chambers S A, Heald S M and Droubay T 2003 *Phys. Rev.* B **67** 100401(R)
[17] Yadav H K, Sreenivas K and Gupta V 2006 *J. Appl. Phys.* **99** 083507
[18] Saeki H, Matsui H, Kawai T and Tabata H 2004 *J. Phys.: Condens. Matter* **16** S5533
[19] Yuan G D, Ye Z Z, Zhu L P, Zeng Y J, Huang J Y, Qian Q and Lu J G 2004 *Mater. Lett.* **58** 3741
[20] Burstein E 1953 *Phys. Rev.* **93** 632
[21] Pearton S J, Heo W H, Ivill M, Norton D P and Steiner T 2004 *Semicond. Sci. Technol.* **19** R59
[22] Xu X H, Blythe H J, Ziese M, Behan A J, Neal J R, Mokhtari A, Ibrahim R M, Fox A M and Gehring G A 2006 *New J. Phys.* **8** 135
[23] Liu X J, Song C, Zeng F, Wang X B and Pan F 2007 *J. Phys. D: Appl. Phys.* **40** 1608
[24] Venkatesan M, Fitzgerald C B and Coey J M D 2004 *Nature* **430** 630
[25] Song C, Pan S N, Liu X J, Zeng F, Yan W S, He B and Pan F 2007 *J. Phys.: Condens. Matter* **19** 176229
[26] Coey J M D, Venkatesan M and Fitzgerald C B 2005 *Nat. Mater.* **4** 173